Mechanism of dust-acoustic instability in a direct current glow discharge plasma

V. E. Fortov, A. G. Khrapak, S. A. Khrapak,[a] V. I. Molotkov, A. P. Nefedov, O. F. Petrov, and V. M. Torchinsky
High Energy Density Research Center, Russian Academy of Sciences, Izhorskaya 13/19, 127412 Moscow, Russia

(Received 25 October 1999; accepted 20 January 2000)

An observation of low frequency waves spontaneously excited in a dc glow discharge dusty plasma is reported. To analyze possible reasons for the instability observed, a linear dispersion relation which takes into account collisions with neutrals, dust grain charge variations, ion drift, and forces acting on dust particles is derived. Numerical analysis of the dispersion relation shows that the observed instability is the result of dust charge variations in the presence of external charge-dependent forces together with the ion drift effect. © *2000 American Institute of Physics.* [S1070-664X(00)01005-3]

I. INTRODUCTION

In recent years there has been much interest in new wave behavior that results from the presence of charged dust particles in plasmas. The dust particles are generally extremely massive and multiply charged as compared to plasma ions (for example, the charge number Z_d of an isolated spherical particle when emission processes are unimportant can be estimated as $Z_d \sim aT_e/e^2$, where a is the particle radius, T_e is the electron temperature, giving $Z_d \sim 10^3$ for $a \sim 1\ \mu$m, and $T_e \sim 1$ eV). In addition, their charge is not fixed, but is coupled self-consistently to the surrounding plasma parameters. For this reason various new wave modes can exist in dusty plasmas, ranging from modifications of well-known plasma waves and instabilities to new ones, such as the dust-acoustic wave (DAW), first considered theoretically by Rao, Shukla, and Yu.[1] The inertia in this mode is provided by charged and massive dust particles, and the pressure to sustain the wave is provided by plasma electrons and ions. Physically, the DAW is analogous to the ion acoustic wave in a dust free plasma, but occurs at very low frequency because the dust particles are many orders of magnitude heavier than ions. More recently, DAWs were studied by several authors in different theoretical contexts, including variations of the dust particle's charge in the presence of the wave,[2,3] the dust-acoustic instability driven by ions and/or electrons drifting relatively to charged dust,[4–7] nonlinearity effects,[8–10] the effect of strongly coupled dusty plasmas,[11–13] as well as the effects of ionization and ion drag.[14–17]

Experimental observations of DAWs in low temperature laboratory plasma devices with trapped dust particles have also been reported.[18–21] This mode can be analyzed easily in experiments by recording the scattered laser light, which illuminates the particle cloud, on a video tape. Even with the naked eye, the dust density fluctuations of very low frequency can often be observed. In Ref. 21, DAW was excited by means of a wire situated near the particles' cloud and driven by a sinusoidal voltage source. The measured dispersion relation yields experimental values for the dust particle charge and plasma Debye length. In other experiments, the dust density fluctuations[18–20,22–24] or individual particle vibrations[25] on slow time scales were spontaneously excited, indicating some kind of instabilities. One of the possible driving mechanisms of DAW is the ion–dust streaming instability,[4–7] which arises as a result of ions motion relative to the levitating dust grains and can be important in different laboratory devices.[18,19,24]

In the DAW frequency limit $\omega \ll k v_{T_e}$, $|\omega - k u_i| \ll k v_{T_i}$, $\omega \gg k v_{T_d}$, the dispersion relation which takes ion drift into account reads[5,24]

$$1+\frac{1}{k^2\lambda_{\rm D}^2}+i\sqrt{\frac{\pi}{2}}\frac{\omega-ku_i}{k^3\lambda_{{\rm D}i}^2 v_{T_i}}-\frac{\omega_{pd}^2}{\omega^2}\cong 0, \quad (1)$$

where ω and k are the wave frequency and number, respectively, $v_{T_\alpha}=\sqrt{T_\alpha/m_\alpha}$ is the thermal velocity of a specie α (α equals e for the electrons, i for the ions, and d for the dust grains), $u_{e(i)}$ is the drift velocity of electrons (ions), $\lambda_{{\rm D}e(i)}=\sqrt{T_{e(i)}/4\pi e^2 n_{e(i)}}$ is the electron (ion) Debye length ($\lambda_{\rm D}^{-2}=\lambda_{{\rm D}e}^{-2}+\lambda_{{\rm D}i}^{-2}$), and $\omega_{pd}=\sqrt{4\pi Z_d^2 e^2 n_d/m_d}$ is the dust plasma frequency. In deriving Eq. (1) we have neglected all collisions with neutrals, damping due to variations of the dust grain charge in the presence of the wave,[3] and the dust Landau damping term. Thus, instability occurs if the ion drift velocity exceeds the wave phase velocity $u_i > \omega/k$. Assuming $\omega=\omega_r+i\gamma$ ($\omega_r \gg \gamma$) and neglecting ω as compared to ku_i, we can obtain the following expressions for the real ω_r and imaginary γ parts of the DAW frequency:

$$\omega_r=\frac{\omega_{pd}k\lambda_{\rm D}}{(1+k^2\lambda_{\rm D}^2)^{1/2}}, \qquad \gamma=\omega_{pd}\sqrt{\frac{\pi}{8}}\frac{u_i}{v_{T_i}}\left(\frac{\lambda_{\rm D}}{\lambda_{{\rm D}i}}\right)^2\frac{k\lambda_{\rm D}}{(1+k^2\lambda_{\rm D}^2)^{3/2}}. \quad (2)$$

The growth rate as a function of k reaches its maximum value

[a]Electronic mail: skhrapak@mail.ru

$$\gamma_{\max}=\frac{\omega_{pd}}{3}\sqrt{\frac{\pi}{6}}\left(\frac{\lambda_{\mathrm{D}}}{\lambda_{\mathrm{D}i}}\right)^2\frac{u_i}{\nu_{T_i}}$$

at $k\lambda_{\mathrm{D}}=1/\sqrt{2}$ and $\omega_r=\omega_{pd}/\sqrt{3}$. These are parameters that correspond to the most effective development of the instability. Collisions with neutrals and charge variations lead to a decrease of the growth rate.

In this paper we report the observation of low-frequency waves spontaneously excited in a dc glow discharge dusty plasma. We show that the previous interpretation of this effect,[24] based on the ion–dust streaming instability [and the dispersion relation (1)] was not sufficiently correct. It is shown that the ion–dust streaming instability alone cannot be responsible for the phenomenon observed because the driving mechanism of this instability is not effective enough as compared to damping (collisional and collisionless due to charge variations) in our conditions. The damping effects were absent in the previous model.[24]

However, we propose a completely new mechanism of DAW instability and compare it with the experimental results. The instability mechanism is based on the dust charge perturbations, as well as on the nature of the forces that trap dust particles within the discharge camera. The point is that in laboratory plasma devices dust particles can be trapped within the plasma region by the balance between all forces that act on them. The most important forces are gravitational, electric, and ion drag. Thus the net force (which has to be zero within the balancing region) usually depends on the dust particle charge. As will be shown, the charge variations in the presence of the wave not only damp the wave but lead to variations in the net force. These periodic variations of the net force can lead, in turn, to the parametric amplification of the wave resulting in DAW instability. Note that although the presence of an electric field and/or ion drift are the necessary conditions for the present instability, the latter is not a modification of the ion–dust streaming instability but is an entirely new type of instability which has no analog in dust free plasmas.

This paper is organized in the following fashion. In Sec. II we describe our experimental setup, summarize some basic plasma and dust parameters, and present the experimental observation of the low-frequency DAW. In Sec. III the model describing the DAW instability in the presence of dust grain charge variations and charge-dependent forces is introduced. The general dispersion relation for this mode is obtained and analyzed. In Sec. IV we compare our results with the experimental ones. In Sec. V we briefly summarize our findings.

II. EXPERIMENTAL RESULTS

A dc glow discharge was created in neon in a cylindrical vertically positioned tube with cold electrodes. The experimental setup is shown schematically in Fig. 1. It was practically the same as had been used in our previous works.[26,27] The inner diameter of the tube was 3 cm, the length of the tube was 60 cm, and the distance between the electrodes was 40 cm. The dust particles to be introduced into the plasma (we have used monodisperse melamin formaldehyde spherical particles 1.87 μm in diameter and mass density $\rho=1.5$ g/cm^3) were held in a cylindrical container located in the upper part of the glass discharge tube. The bottom of the container was fashioned from a metal mesh with a spacing of 100 μm. When the container was shaken, particles rained down into the positive column of the discharge. Some of them were found to be trapped in a discharge region where there is a balance between the forces acting on them. They could be seen as a cloud levitated in the center of the tube. Observations were made by illuminating a vertical plane with a sheet of a laser light. The scattered laser light was recorded by a video camera.

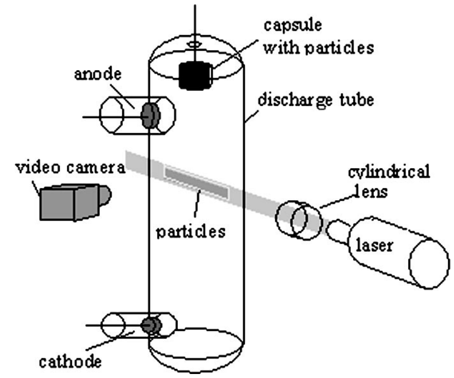

FIG. 1. Schematic representation of the experimental setup.

Under some conditions low-frequency perturbations of the dust number density propagating downwards (from the anode to the cathode) were observed. They were excited spontaneously as a result of either reducing the neutral gas pressure or the discharge current. Injection of new particles in the discharge can also lead to wave excitation. A typical wave pattern is shown in Fig. 2. The wave number and the phase velocity found from a succession of pictures of this type are $k=2\pi/L\sim 60\,\mathrm{cm}^{-1}$ and $\nu_{\mathrm{ph}}\sim 1$ cm/s, where L is the wavelength. This results in the wave frequency $\omega=k\nu_{\mathrm{ph}}\sim 60\,\mathrm{s}^{-1}$. The spontaneous excitation of such waves in a similar experiment was first described in Ref. 24.

For further analysis, knowledge of the main dusty plasma parameters is needed. Some of them are relatively well known and can even be controlled during the experiment. For example, dust particle size and mass are known. Neutral gas pressure and discharge current are controlled during the experiment. Dust particles number density can be approximately determined through average interparticle distance when no waves exist. The other parameters can be calculated using some model approaches, and are, therefore, less certain. We expect the values of basic plasma parameters to be similar to those of a typical small current dc glow discharge: electron temperature $T_e\sim 3$ eV, ion and neutral gas temperature $T_i\sim T_n\sim 0.03$ eV, electron and ion number densities n_e, $n_i\sim 10^7-10^8\,\mathrm{cm}^{-3}$, the vertical electric field in the positive column directed downwards is $E\sim 1$ V/cm. In such a small electric field the electron drift velocity is given by

$$u_e=-eE/m_e\nu_{en}, \tag{3}$$

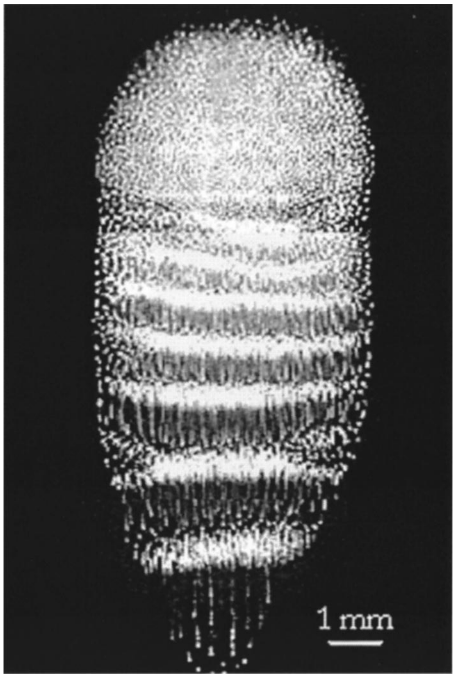

FIG. 2. Typical dust acoustic wave video image. Neutral gas pressure $P \sim 0.2$ Torr.

where $\nu_{en} \sim n_n \sigma_{en} \nu_{T_e}$ is the frequency of the electron–neutral collisions, n_n is the neutral number density, and $\sigma_{en} \sim 2\times 10^{-16}\,\mathrm{cm}^{-2}$ is the electron–neutral collisional cross section for neon. The ions' equilibrium drift velocity is

$$u_i = \mu_i E, \tag{4}$$

where $\mu_i \sim 3\times 10^3\, E/P\,[\mathrm{cm}^2\,\mathrm{Torr}/(\mathrm{s\,V})]$ is the mobility of Ne^+ in Ne.[28]

In discharge plasma conditions, dust particles are charged negatively due to electron and ion collection. The steady state charge is determined by the condition $I_e = I_i$, where $I_{e(i)}$ is the electron (ion) plasma flux to the particle surface. Within the framework of the standard orbit motion limited approach,[29] these fluxes are given by

$$I_e = \sqrt{8\pi} a^2 n_e \nu_{T_e} \exp\left(\frac{Z_d e^2}{a T_e}\right), \tag{5}$$

$$I_i = \sqrt{8\pi} a^2 n_i \nu_{T_i}\left(1 - \frac{Z_d e^2}{a T_i}\right). \tag{6}$$

To evaluate the grains charge in the region of dust cloud the quasineutrality condition

$$n_e = n_i + Z_d n_d \tag{7}$$

has to be used together with Eqs. (5) and (6). Equation (7) takes into account the possible effect of electron depletion in the dust cloud if dust particles' number density is sufficiently high.

To conclude this section we analyze the forces acting on the dust particles that can be important in our experiment. The charged dust particles are trapped, and levitate in a region where the sum of all forces acting on them is zero. In the radial direction, they are confined by a radial discharge electric field. In the vertical direction, the main forces to be considered are: the gravitational force, the electric force due to a vertical discharge electric field, and the ion drag force. The electric force directed upwards is $F_e \cong Z_d e E$. The forces directed downwards are the gravitational force $F_g = m_d g$ and the ion drag one. Estimations show that for our typical plasma parameters and $u_i < \nu_{T_i}$ the force experienced by the particles due to drifting ions is more than one order of magnitude less than the force of gravity. Thus, the force balance can be written as

$$F_\Sigma = Z_d e E + m_d g = 0. \tag{8}$$

The force that is important for dust dynamics is the friction with a neutral gas or neutral drag force. For mean free paths of neutral atoms that are large compared to the grain radius and for specular reflection of atoms from the grain surface, the neutral drag force is given by (see, for example, Ref. 30 and references therein)

$$F_{nd} = \frac{8\sqrt{2\pi}}{3} a^2 n_n T_n \frac{\nu_d}{\nu_{T_n}} = m_d \nu_{dn} \nu_d, \tag{9}$$

where $\nu_{dn} = \sqrt{8/\pi}\, n_n T_n/(\nu_{T_n} \rho a)$ and ν_d is the dust particle velocity.

III. DUST ACOUSTIC WAVE MODEL

In this section we discuss a physical effect which (together with the ion–dust streaming instability) can be responsible for the wave excitations in our experiment. First of all, a linear dispersion relation that could be used to predict the imaginary part of the frequency has to be obtained. Collisions with neutrals, charge variations of dust grains, and ion and electron drifts are taken into account. To derive a linear dispersion relation, we use the Poisson's equation for the electrostatic potential of the wave φ,

$$\nabla^2 \varphi = -4\pi e [n_i - n_e + Z_d n_d]. \tag{10}$$

Assuming the small perturbations $n_\alpha = n_{\alpha 0} + n_{\alpha 1}$, $Z_d = Z_{d0} + Z_{d1}$, $\varphi = \varphi_1$ with the $\sim \exp(ikx - i\omega t)$ dependence and using the quasineutrality condition at equilibrium $n_{e0} = n_{i0} + Z_{d0} n_{d0}$ we can linearize Eq. (10):

$$-k^2 \varphi_1 = -4\pi e [n_{i1} - n_{e1} + Z_{d0} n_{d1} + Z_{d1} n_{d0}]. \tag{11}$$

In Eq. (11) the first-order dust charge density consists of the terms $Z_{d0} n_{d1}$ and $Z_{d1} n_{d0}$, which represent the dust-particle-number density and dust-charge-number perturbations, respectively. The dispersion relation can be written in the form

$$1 + \chi_i + \chi_e + \chi_d = 0, \tag{12}$$

where $\chi_i = -4\pi e n_{i1}/k^2 \varphi_1$, $\chi_e = 4\pi e n_{e1}/k^2 \varphi_1$, $\chi_d = -4\pi e (Z_{d0} n_{d1} + Z_{d1} n_{d0})/k^2 \varphi_1$ are the susceptibilities of a corresponding species. The ion and electron number density perturbations in the presence of equilibrium drift and collisions with neutrals can be derived using the standard kinetic approach.[31] This results in

$$\chi_\alpha = k^{-2} \lambda_{\mathrm{D}\alpha}^{-2} [1 - J_+(\xi_\alpha)] \left[1 - \frac{i \nu_{\alpha n}}{\xi_\alpha k \nu_{T_\alpha}} J_+(\xi_\alpha)\right]^{-1}, \tag{13}$$

where $J_+(x)=x\exp(-x^2/2)\int_{i\infty}^{x} d\tau \exp(\tau^2/2)$, $\xi_e=(\omega+ku_e+i\nu_{en})/k\nu_{T_e}$, and $\xi_i=(\omega-ku_i+i\nu_{in})/k\nu_{T_i}$ for a wave propagating in the direction of electric field ($\alpha=e,i$). We consider a situation of small drift velocities $u_{e(i)}<\nu_{T_{e(i)}}$. For electrons $\nu_{en}/k\nu_{T_e}\ll 1$ is also assumed so that $|\xi_e|<1$. Using an approximate expression[31] $J_+(x)\approx -i\sqrt{\pi/2}x$ which is valid for $|x|\ll 1$, Eq. (13) can be reduced to

$$\chi_e\cong k^{-2}\lambda_{\mathrm{De}}^{-2}\left[1+i\sqrt{\frac{\pi}{2}}\frac{\omega+ku_e}{k\nu_{T_e}}\left(1+\sqrt{\frac{\pi}{2}}\frac{\nu_{en}}{k\nu_{T_e}}\right)\right]$$
$$\approx k^{-2}\lambda_{\mathrm{De}}^{-2}\left[1+i\sqrt{\frac{\pi}{2}}\frac{\omega+ku_e}{k\nu_{T_e}}\right]. \quad (14)$$

Thus, collisions with neutrals do not play an important role in the limit $\nu_{en}/k\nu_{T_e}\ll 1$ because the wavelength is less than the mean collision free path of electrons. For collisionless ions we have similarly

$$\chi_i\approx k^{-2}\lambda_{\mathrm{Di}}^{-2}\left[1+i\sqrt{\frac{\pi}{2}}\frac{\omega-ku_i}{k\nu_{T_i}}\right]. \quad (15)$$

In a collisional case, $\nu_{in}/k\nu_{T_i}>1$, Eq. (13) can be numerically calculated to obtain ions susceptibility. However, for simplicity we will use the result obtained by D' Angelo and Merlino using fluid approximation,[7]

$$\chi_i=k^{-2}\lambda_{\mathrm{Di}}^{-2}\left[1+i\nu_{in}\frac{\omega-ku_i}{k^2\nu_{T_i}^2}\right]. \quad (16)$$

Equation (16) is valid when $\nu_{in}|\omega-ku_i|\ll k^2\nu_{T_i}^2$.

The number density perturbations of charged cold dust fluid is determined from the one-dimensional continuity and momentum equations which read, respectively,

$$\frac{\partial n_d}{\partial t}+\frac{\partial}{\partial x}(n_d\nu_d)=0, \quad (17)$$

$$\frac{\partial \nu_d}{\partial t}+\nu_d\frac{\partial \nu_d}{dx}=-\frac{Z_d e}{m_d}\frac{\partial\varphi}{\partial x}+\frac{F_\Sigma}{m_d}-\nu_{dn}\nu_d, \quad (18)$$

where F_Σ is the total force acting on the dust particles in the direction of wave propagation (vertical direction). According to Eq. (8) $F_{\Sigma 0}=0$ and linearization gives $F_{\Sigma 1}=(\partial F_\Sigma/\partial Z_d{}_{Z_{d0}})Z_{d1}=eEZ_{d1}$. Thus, linearized Eqs. (17) and (18) are

$$-i\omega n_{d1}+ikn_{d0}\nu_{d1}=0, \quad (19a)$$

$$(-i\omega+\nu_{dn})\nu_{d1}=-iZ_{d0}ek\varphi_1/m_d+eEZ_{d1}/m_d. \quad (19b)$$

The dust charge perturbation is determined from the equation $\partial Z_d/\partial t=I_i-I_e$. Linearizing it with the help of Eqs. (5) and (6) one can obtain[3]

$$(-i\omega+\eta)Z_{d1}=I_{i0}\left(\frac{n_{i1}}{n_{i0}}-\frac{n_{e1}}{n_{e0}}\right), \quad (20)$$

where

$$\eta=I_{i0}\frac{e^2}{aT_e}[1+(T_i/T_e-Z_{d0}e^2/aT_e)^{-1}]$$

is the natural decay rate of charge fluctuations, $I_{i0}=I_{e0}$ is the unperturbed ion or electron current to the particle surface. Neglecting the small imaginary part in Eqs. (14) and (15) or (16) one can see that the first-order number density perturbations of electrons and ions are given by Boltzmann relations,

$$n_{e1}=n_{e0}\frac{e\varphi_1}{T_e}, \quad n_{i1}=-n_{i0}\frac{e\varphi_1}{T_i}. \quad (21)$$

Substituting (21) into (20) we obtain for dust charge perturbation

$$Z_{d1}=-i\frac{I_{i0}(1+T_e/T_i)}{\omega+i\eta}\frac{e\varphi_1}{T_e}. \quad (22)$$

Thus from Eqs. (17), (18), and (22) we obtain dust susceptibility,

$$\chi_d=-\frac{\omega_{pd}^2}{\omega(\omega+i\nu_{dn})}+i\frac{I_{i0}(1+T_e/T_i)}{k^2\lambda_{\mathrm{De}}^2(\omega+i\eta)}\frac{n_{d0}}{n_{e0}}$$
$$-\frac{\omega_{pd}^2}{\omega(\omega+i\nu_{dn})}\frac{I_{i0}(1+T_e/T_i)eE/T_e}{Z_{d0}k(\omega+i\eta)}. \quad (23)$$

The dispersion relation can be constructed using (12), (14), (23), and (15) or (16) depending on the value of $\nu_{in}/k\nu_{T_i}$.

Some analysis of the obtained dispersion relation is in order. We assume that the real part of the frequency is close to DAW dispersion given by Eq. (2) and examine the influence of the effects considered on the imaginary part of the frequency. It is clear that the dust–neutral collisions lead to the damping of DAW. The damping rate is $\gamma_{dc}\sim -v_{dn}/2$. The Landau damping on electrons is

$$\gamma_{\mathrm{Le}}\sim -\omega_{pd}\frac{k\lambda_{\mathrm{D}}}{(1+k^2\lambda_{\mathrm{D}}^2)^{3/2}}\frac{\lambda_{\mathrm{D}}^2}{\lambda_{\mathrm{De}}^2}\frac{\omega+ku_e}{k\nu_{T_e}} \quad (24)$$

and is increased due to electron drift in the direction opposite to wave propagation. The effect is small because as usual $\lambda_{\mathrm{De}}\gg\lambda_{\mathrm{D}}\sim\lambda_{\mathrm{D}i}$. The Landau damping on ions changes a sign when the ion drift velocity exceeds the wave phase velocity and leads to instability. In the collisionless limit, the growth rate is given by Eq. (2). When collisions are of importance the growth rate is

$$\gamma_{\mathrm{Li}}\sim -\omega_{pd}\frac{k\lambda_{\mathrm{D}}}{(1+k^2\lambda_{\mathrm{D}}^2)^{3/2}}\frac{\lambda_{\mathrm{D}}^2}{\lambda_{\mathrm{Di}}^2}\frac{\omega-ku_i}{k\nu_{T_i}}\frac{\nu_{in}}{k\nu_{T_i}}. \quad (25)$$

Charge variations in the absence of external forces acting on dust particles and in a plasma without any anisotropy [the second term on the right hand side (RHS) of Eq. (23)] lead to the damping of DAW. In the limit $\omega\gg\eta$ the damping rate becomes

$$\gamma_{\mathrm{ch}}=-\frac{\beta}{2(1+k^2\lambda_{\mathrm{D}}^2)}, \quad (26)$$

where

TABLE I. Basic plasma/dust parameters.

Dust grain radius	$a=0.94\ \mu$m
Dust grain concentration	$n_d=5\times10^4$ cm^{-3}
Ion concentration	$n_i=10^8$ cm^{-3}
Dust grain mass	$m_d=5.2\times10^{-12}$ g
Dust grain charge	$Z_d\sim-1.8\times10^3$
Electron concentration	$n_e\sim1.2\times10^7$ cm^{-3}
Discharge electric field	$E\sim1.8$ V/cm
Plasma–dust frequency	$\omega_{pd}\sim290$ s^{-1}
Plasma ion Debye length	$\lambda_{Di}\sim0.013$ cm
Plasma electron Debye length	$\lambda_{De}\sim0.38$ cm
Plasma Debye length	$\lambda_D\sim0.013$ cm
Electron thermal velocity	$v_{T_e}\sim7.3\times10^7$ cm/s
Ion and neutral thermal velocity	$v_{T_i}\sim v_{T_n}\sim4\times10^4$ cm/s
Plasma ion flux to the particle surface	$I_{i0}\sim1.5\times10^7$ s^{-1}

$$\beta=I_{i0}(1+T_e/T_i)\frac{\lambda_D^2}{\lambda_{De}^2}\frac{n_{d0}}{n_{e0}}.$$

The same result (for $k^2\lambda_D^2\ll1$) has been obtained in Ref. 3. However, in a laboratory dusty plasma the other limiting case $\omega\ll\eta$ is often realized. In this limit the damping rate is

$$\gamma_{ch}\sim-\frac{\beta}{2}\left(\frac{\omega_{pd}}{\eta}\right)^2\frac{k^2\lambda_D^2}{[1+k^2\lambda_D^2+\beta/\eta]^2}. \quad (27)$$

Finally, the last term on the rhs of Eq. (23) is due to both dust charge variations and charge-dependent external forces that trap the particles. In the limit $\omega\ll\eta$ we obtain that DAW becomes unstable. The growth rate of this instability is

$$\gamma_{ef}\sim-\frac{\omega_{pd}}{2}\frac{Z_{d0}eE\lambda_D}{T_e}\frac{I_{i0}(1+T_e/T_i)}{Z_{d0}^2\eta(1+k^2\lambda_D^2)^{1/2}} \quad (28)$$

(note that $Z_{d0}<0$). Physically, the DAW becomes unstable because, in conditions considered here, an additional periodic force (associated with charge variations) acting on the trapped dust particles is in phase with their velocity that can be seen from Eqs. (19b) and (22). This periodic force performs positive work on the dust particles during the wave period leading to the parametric amplification of the wave.

We can summarize that the ion drift leads to the DAW instability but dust–neutral collisions and electron drift lead to the damping of DAW. Dust charge variations may lead to both wave damping and growth. The collisionless damping of DAW due to charge variations is *always* present in dusty plasma. On the other hand, in the presence of external charge-dependent forces, charge variations can also be a cause of the DAW instability.

IV. COMPARISON WITH EXPERIMENTAL RESULTS

Dispersion relation (12) together with expressions (14)–(16), and (23) can be analyzed numerically for a given set of plasma and dust parameters. To compare the conditions for DAW instability resulting from Eq. (12) with experiment, we fix basic plasma parameters to be close to experimental ones, e.g., we chose $n_i=10^8$ cm^{-3}, $n_d=5\times10^4$ cm^{-3}. All other dust/plasma parameters can be calculated using Eqs. (5)–(8). These plasma parameters are summarized in Table I. The main difficulty is to distinguish between the collisionless and collisional regimes for ions, as in the range of pressures where the instability takes place the mean free path for ion–neutral charge exchange collisions is comparable to the wavelength of the mode observed. For example, characteristic frequencies and drift velocities calculated for $P=0.2$ Torr and $P=0.3$ Torr are given in Table II. One can see that for $P=0.2$ Torr the condition $\nu_{in}/kv_{T_i}<1$ holds for $k\gtrsim25$ cm^{-1}. Thus, Eq. (15) can be used if the wave mode with $k\gtrsim25$ cm^{-1} is considered. On the other hand, for $P=0.3$ Torr the collisional expression for ions susceptibility (16) have to be used in the range 15 cm$^{-1}\lesssim k\lesssim40$ cm^{-1}.

TABLE II. Characteristic frequencies and drift velocities.

	$P=0.2$ Torr	$P=0.3$ Torr
Frequency of dust–neutral collisions	$\nu_{dn}\sim80$ s^{-1}	$\nu_{dn}\sim120$ s^{-1}
Frequency of ion–neutral collisions	$\nu_{in}\sim10^6$ s^{-1}	$\nu_{in}\sim1.6\times10^6$ s^{-1}
Frequency of electron–neutral collisions	$\nu_{en}\sim8\times10^7$ s^{-1}	$\nu_{en}\sim1.2\times10^8$ s^{-1}
Ion drift velocity	$u_i=2.7\times10^4$ cm/s	$u_i=1.8\times10^4$ cm/s
Electron drift velocity	$u_e=4\times10^7$ cm/s	$u_e=2.7\times10^7$ cm/s

The real and imaginary parts of DAW frequency versus wave number k for two different neutral gas pressures are shown in Figs. 3 and 4. These figures show that the effect of charge variations of trapped dust particles together with the ion drift leads to wave instability in the conditions considered. The instability growth rate as a function of k has a pronounced maximum. This mode as the most unstable can be excited in experiment. For $P=0.2$ Torr the maximum is reached at $k\cong60$ cm^{-1}. The frequency of this mode determined using curve 1 in Fig. 3 is $\omega\cong130$ s^{-1}. A similar wave mode ($k\sim60$ cm^{-1}, $\omega\sim60$ s^{-1}) was observed in our experiment. It is unreasonable to expect more precise quantitative agreement for a large number of reasons. First of all, there exists some arbitrariness in choosing plasma parameters, which are not measured directly during the experiment. Second, the model considered contains some simplifications discussed in the following.

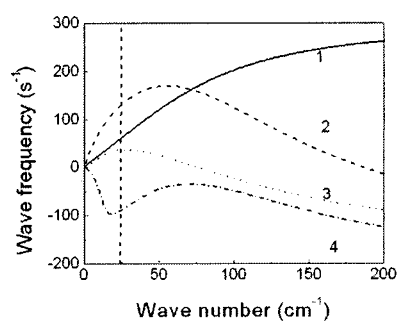

FIG. 3. Numerical solution of Eq. (12) for $P=0.2$ Torr. Curve 1 shows Re $\omega(k)$, curve 2 shows Im $\omega(k)\times5$ for parameters listed in Tables I and II. Curves 3 and 4 are Im $\omega(k)\times5$ obtained as a result of substitution $u_i=0$ and $E=0$ into Eqs. (15) and (23), respectively, for the same set of the other parameters. The vertical dashed line shows the condition $k>25$ cm^{-1} when the collisionless approach for ions can be used.

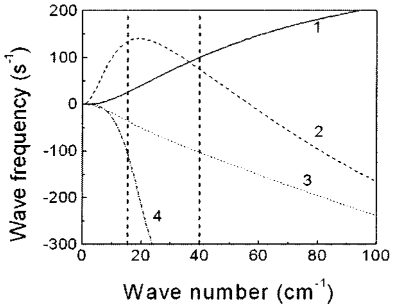

FIG. 4. Numerical solution of Eq. (12) for $P=0.3$ Torr. Curve 1 shows Re $\omega(k)$, curve 2 shows Im $\omega(k)\times 5$ for parameters listed in Tables I and II. Curves 3 and 4 are Im $\omega(k)\times 5$ obtained as a result of substitution $u_i=0$ and $E=0$ into Eqs. (16) and (23), respectively, for the same set of the other parameters. Vertical dashed lines show the condition $15\,\mathrm{cm}^{-1}<k<40\,\mathrm{cm}^{-3}$ when the collisional expression (16) for ions can be used.

Note that the mechanism of instability associated with charge variations in the presence of external forces that trap dust particles is effective itself in the conditions considered. The role of ion drift, which cannot lead to wave instability (see Fig. 3), is to transpose the maximum increment of instability to the largest values of k (and consequently ω). As ions are always drifting in an external electric field, both mechanisms are always indivisible and their relative efficiency can vary in various plasma conditions. However, the instability considered in this paper is not a modification of the known ion–dust streaming instability but represents an entirely new one.

For higher pressures neither the effect of charge variations in the presence of the external forces nor the effect of ion drift can lead to wave instability. However, the sum of these effects results in the instability with the characteristics of the most unstable mode $k\sim 20\,\mathrm{cm}^{-1}$ and $\omega\sim 40\,\mathrm{s}^{-1}$ (see Fig. 4).

The dispersion relation (12) together with the model approaches used in Sec. II allows us to explain all the qualitative peculiarities found in the experiment. For example, the wave disappears with an increase of neutral gas pressure. This is the result of an increase of the collisional damping introduced by dust-neutral collisions. Numerical analysis of Eq. (12) shows that for $n_i\sim 10^8\,\mathrm{cm}^{-3}$ and $n_d\sim 5\times 10^4\,\mathrm{cm}^{-3}$ the critical value of pressure for which Im $\omega(k)$ becomes negative for all values of k is approximately 0.5 Torr. Moreover, with increasing the neutral gas pressure the wavelength of the most unstable mode also increases (see Fig. 4). This means that the wave will disappear when the wavelength becomes comparable to the size of the dust cloud.

The wave can be excited as a result of injection of new particles in the discharge tube leading to the increase of dust number density. Numerical analysis shows that for $n_i\sim 10^8\,\mathrm{cm}^{-3}$ and neutral gas pressure 0.2 Torr DAW instability occurs for $n_d\gtrsim 2\times 10^4\,\mathrm{cm}^{-3}$.

The wave also disappears when increasing the discharge current. We attribute this to the increase of plasma ion and electron number densities and decrease in ion and electron Debye lengths. Numerical analysis of the model shows that this is accompanied by a decrease in the electric field and increase in the particles charge and charging frequency. When all these effects are taken into account, we see that with the increase of n_i the most unstable mode moves to the region of very large values of k (see Fig. 5) and at smaller values of k the wave becomes damped. However, the DAW can exist only if the interparticle distance is sufficiently less than the wavelength of the mode. This gives a simple evaluation $k\lesssim 2\pi n_d^{1/3}\sim 250\,\mathrm{cm}^{-1}$ for $n_d\sim 5\times 10^4\,\mathrm{cm}^{-3}$.

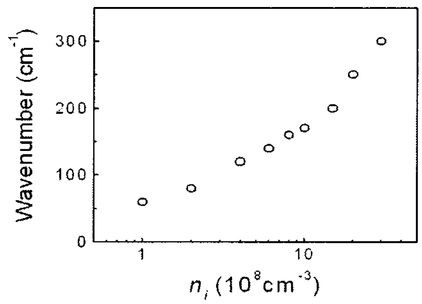

FIG. 5. The wave number of the most unstable mode as a function of ion number density found from numerical analysis of Eq. (12). The neutral gas pressure is 0.2 Torr and the collisionless expression (15) for ions susceptibility is used.

Finally, we summarize some simplifications of our analytical model. First of all, we have derived a linear dispersion relation to predict the onset of the instability. However, this approach is insufficient to explain the actual experimental observations where highly nonlinear waves were observed (see Fig. 2). Second, a spatial inhomogeneity of a plasma was not taken into account. At the same time the discharge was stratified in our experiment and the instability was observed in a dust cloud region which is supported by the head of the striation. The latter region is highly inhomogeneous. Third, the dusty plasma nonideality was also not taken into account, although the coupling parameter evaluated for $T_d=0.03\,\mathrm{eV}$ is very high

$$\Gamma_d=\frac{Z_d^2e^2n_d^{1/3}}{T_d}\sim 500.$$

However, the effect of anomalous dust particle heating found in experiments[21,26,32–34] and considered recently theoretically[35–37] can decrease Γ_d by several orders of magnitude.

V. CONCLUSIONS

The observation of the low-frequency waves spontaneously excited in a dc glow discharge dusty plasma is described. To analyze possible reasons for such excitation, a linear dispersion relation which takes into account collisions with neutrals, dust grain charge variations, ion drift, and forces acting on dust particles is derived. It is shown that the observed instability is the result of dust charge variations in the presence of external charge-dependent forces together with the ion drift effect. The results of a numerical analysis of the dispersion relation are in agreement with experimental results.

The mechanism of instability presented in this paper has no analogs in a dust free plasma. The class of plasmas where this mechanism is likely to play a role includes different plasma processing discharges and plasma crystal experiments under gravity conditions, which both involve a particle cloud levitated in a gas discharge plasma due to the balance of electric force and the force of gravity.

ACKNOWLEDGMENTS

This work was supported by the Russian Foundation for Basic Research, Grant Nos. 99-02-18126 and 98-02-16828. The authors are grateful to an unknown referee for useful comments.

[1] N. N. Rao, P. K. Shukla, and M. Y. Yu, Planet. Space Sci. **38**, 543 (1990).
[2] R. K. Varma, P. K. Shukla, and V. Krishan, Phys. Rev. E **47**, 3612 (1993).
[3] M. R. Jana, A. Sen, and P. K. Kaw, Phys. Rev. E **48**, 3930 (1993).
[4] M. Rosenberg, Planet. Space Sci. **41**, 229 (1993).
[5] M. Rosenberg, in *Physics of Dusty Plasmas*, edited by P. K. Shukla, D. A. Mendis, and V. W. Chow (World Scientific, Singapore, 1996), p. 129.
[6] M. Rosenberg, J. Vac. Sci. Technol. A **14**, 631 (1996).
[7] N. D'Angelo and R. L. Merlino, Planet. Space Sci. **44**, 1593 (1996).
[8] N. N. Rao, J. Plasma Phys. **59**, 561 (1998).
[9] J. X. Ma and J. Liu, Phys. Plasmas **4**, 253 (1997).
[10] D. Winske and M. Rosenberg, IEEE Trans. Plasma Sci. **26**, 92 (1998).
[11] M. Rosenberg and G. Kalman, Phys. Rev. E **56**, 7166 (1997).
[12] M. S. Murillo, Phys. Plasmas **5**, 3116 (1998).
[13] D. Winske, M. S. Murillo, and M. Rosenberg, Phys. Rev. E **59**, 2236 (1999).
[14] P. K. Shukla and G. Morfill, Phys. Lett. A **216**, 153 (1996).
[15] N. D'Angelo, Phys. Plasmas **4**, 3422 (1997).
[16] N. D'Angelo, Phys. Plasmas **5**, 3155 (1998).
[17] A. V. Ivlev, D. Samsonov, J. Goree, G. Morfill, and V. E. Fortov, Phys. Plasmas **6**, 741 (1999).
[18] A. Barkan, R. L. Merlino, and N. D'Angelo, Phys. Plasmas **2**, 3536 (1995).
[19] R. L. Merlino, A. Barkan, C. Thompson, and N. D'Angelo, Phys. Plasmas **5**, 1607 (1998).
[20] H. R. Prabhakara and V. L. Tana, Phys. Plasmas **3**, 3176 (1996).
[21] J. B. Pieper and J. Goree, Phys. Rev. Lett. **77**, 3137 (1996).
[22] J. H. Chu, J. B. Du, and L. I, J. Phys. D **27**, 296 (1994).
[23] D. Samsonov and J. Goree, Phys. Rev. E **59**, 1047 (1999).
[24] V. I. Molotkov, A. P. Nefedov, V. M. Torchinsky, V. E. Fortov, and A. G. Khrapak, Zh. Eksp. Teor. Fiz. **116**, 902 (1999) (in Russian) [JETP **89**, 477 (1999)].
[25] S. Nunomura, T. Misawa, N. Ohno, and S. Takamura, Phys. Rev. Lett. **83**, 1970 (1999).
[26] V. E. Fortov, A. P. Nefedov, V. M. Torchinsky, V. I. Molotkov, O. F. Petrov, A. A. Samarian, A. M. Lipaev, and A. G. Khrapak, Phys. Lett. A **229**, 317 (1997).
[27] A. M. Lipaev, V. I. Molotkov, A. P. Nefedov, O. F. Petrov, V. M. Torchinskii, V. E. Fortov, A. G. Khrapak, and S. A. Khrapak, Zh. Eksp. Teor. Fiz. **112**, 2030 (1997) (in Russian) [JETP **85**, 1110 (1997)].
[28] Yu. P. Raizer, *Gas Discharge Physics* (Springer, Berlin, 1991).
[29] J. Goree, Plasma Sources Sci. Technol. **3**, 400 (1994).
[30] J. E. Daugherty and D. B. Graves, J. Appl. Phys. **78**, 2279 (1995).
[31] A. F. Alexandrov, L. S. Bogdankevich, and A. A. Rukhadze, *Principles of Plasma Electrodynamics* (Springer, New York, 1984).
[32] H. Thomas and G. E. Morfill, Nature (London) **379**, 806 (1996).
[33] G. E. Morfill, H. M. Thomas, U. Konopka, and M. Zuzic, Phys. Plasmas **6**, 1769 (1999).
[34] A. Melzer, A. Homann, and A. Piel, Phys. Rev. E **53**, 2757 (1996).
[35] V. Zhakhovskii, V. Molotkov, A. Nefedov, V. Torchinskii, A. Khrapak, and V. Fortov, Pis'ma Zh. Eksp. Teor. Fiz. **66**, 392 (1997) [JETP Lett. **66**, 419 (1997)].
[36] V. A. Schweigert, I. V. Schweigert, A. Melzer, A. Homann, and A. Piel, Phys. Rev. Lett. **80**, 5345 (1998).
[37] O. S. Vaulina, S. A. Khrapak, A. P. Nefedov, and O. F. Petrov, Phys. Rev. E **60**, 5959 (1999).